Study of spin-isospin responses of radioactive nuclei with the background-reduced neutron spectrometer, PANDORA

Stuhl, L.; Sasano, M.; Gao, J.; Hirai, Y.; Yako, K.; Wakasa, T.; Ahn, D. S.; Baba, H.; Chilug, A. I.; Franchoo, S.

Published in:
Nuclear Instruments & Methods in Physics Research Section B-Beam Interactions with Materials and Atoms

DOI:
10.1016/j.nimb.2019.05.057

Nuclear Inst. and Methods in Physics Research B 463 (2020) 189–194

Contents lists available at ScienceDirect

Nuclear Inst. and Methods in Physics Research B

journal homepage: www.elsevier.com/locate/nimb

Study of spin-isospin responses of radioactive nuclei with the background-reduced neutron spectrometer, PANDORA

L. Stuhl[a,b,*], M. Sasano[b], J. Gao[b,c], Y. Hirai[d], K. Yako[a], T. Wakasa[d], D.S. Ahn[b], H. Baba[b], A.I. Chilug[e,f,b], S. Franchoo[g], Y. Fujino[h], N. Fukuda[b], J. Gibelin[i], I.S. Hahn[j], Z. Halász[k], T. Harada[l], M.N. Harakeh[m,n], D. Inomoto[d], T. Isobe[b], H. Kasahara[d], D. Kim[o], G.G. Kiss[k], T. Kobayashi[p], Y. Kondo[q], Z. Korkulu[b], S. Koyama[r], Y. Kubota[b], A. Kurihara[q], H.N. Liu[s], M. Matsumoto[q], S. Michimasa[a], H. Miki[q], M. Miwa[t,b], T. Motobayashi[b], T. Nakamura[q], M. Nishimura[b], H. Otsu[b], V. Panin[b], S. Park[j], A.T. Saito[q], H. Sakai[b], H. Sato[b], T. Shimada[q], Y. Shimizu[b], S. Shimoura[a], A. Spiridon[e], I.C. Stefanescu[e,f], X. Sun[b,c], Y.L. Sun[s], H. Suzuki[b], E. Takada[u], Y. Togano[h], T. Tomai[q,b], L. Trache[e], D. Tudor[e,f,b], T. Uesaka[b], H. Yamada[q], Z. Yang[b], M. Yasuda[q], K. Yoneda[b], K. Yoshida[b], J. Zenihiro[b], N. Zhang[v,a]

[a] Center for Nuclear Study, University of Tokyo, 2-1 Hirosawa, Wako, Saitama, Japan
[b] RIKEN Nishina Center, 2-1 Hirosawa, Wako, Saitama, Japan
[c] School of Physics, Peking University, Beijing 100871, China
[d] Department of Physics, Kyushu University, Motooka 744, Fukuoka, Nishi, Japan
[e] Horia Hulubei National Institute of Physics and Nuclear Engineering, Str. Reactorului 30, Bucharest – Magurele, Romania
[f] Faculty of Physics, University of Bucharest, Str. Atomistilor 405, Magurele 077125, Romania
[g] Institut de Physique Nucleáire, CNRS-IN2P3, UniversitePáris-Sud, UniversitePáris-Saclay, 91406 Orsay Cedex, France
[h] Department of Physics, Rikkyo University, Tokyo 171-8501, Japan
[i] LPC CAEN, ENSICAEN, 6 bd Marüchal Juin, 14050 Caen, Cedex, France
[j] Department of Physics, Ewha Womans University, 120-750 Seoul, Republic of Korea
[k] ATOMKI, Institute for Nuclear Research, Hungarian Academy of Sciences, P. O. Box 51, H-4001 Debrecen, Hungary
[l] Department of Physics, Toho University, 5-21-16 Omorinishi Ota, 143-8540 Tokyo, Japan
[m] KVI – CART, University of Groningen, Zernikelaan 25, 9747 AA Groningen, The Netherlands
[n] GSI Helmholtzzentrum für Schwerionenforschung GmbH, Planckstrasse 1, 64291 Darmstadt, Germany
[o] Department of Physics, Korea University, 02841 Seoul, Republic of Korea
[p] Department of Physics, Tohoku University, Miyagi 980-8578, Japan
[q] Department of Physics, Tokyo Institute of Technology, 2-12-1 O-Okayama, Meguro, Tokyo 152-8551, Japan
[r] Department of Physics, University of Tokyo, Tokyo 113-0033, Japan
[s] Département de Physique Nucléaire, IRFU, CEA, Université Paris-Saclay, F-91191 Gif-sur-Yvette, France
[t] Department of Physics, Saitama University, Shimo-Okubo 255, Sakura, Saitama 338-8570, Japan
[u] National Institute of Radiological Sciences, 4-9-1 Anagawa, Inage, Chiba 263-0024, Japan
[v] Institute of Modern Physics, Chinese Academy of Sciences, Lanzhou 730000, China

ARTICLE INFO

Keywords:
Spin-isospin response
Gamow-Teller transition
Inverse-kinematics (p, n) reactions
Low-energy neutron detector
Real-time pulse-shape discrimination
Figure-of-Merit (FoM)

ABSTRACT

The status of a project to measure spin-isospin responses of neutron drip-line nuclei using a new low-energy neutron detector, PANDORA (Particle Analyzer Neutron Detector Of Real-time Acquisition), is reported. The performance of PANDORA was characterized by the ^{6}He$(p, n)^{6}$Li reaction in inverse kinematics at the HIMAC facility in Chiba. Observation of the strong transition to the ground state in ^{6}Li is discussed. Preliminary results of ^{11}Li$(p, n)^{11}$Be and ^{14}Be$(p, n)^{14}$B experiments in inverse kinematics at RI Beam Factory (RIBF) of RIKEN Nishina Center are also presented including the exotic decay channel of ^{11}Be→^{9}Li + d. Details of the experimental setup based on PANDORA and the SAMURAI large-acceptance magnetic spectrometer, as well as the combined data-acquisition system are described. The neutron-gamma discrimination capability of PANDORA was evaluated, Figure-of-Merit (FoM) values higher than those found in the literature for similar materials were derived from experimental data.

* Corresponding author at: Center for Nuclear Study, University of Tokyo, 2-1 Hirosawa, Wako, Saitama, Japan.
E-mail address: stuhl@cns.s.u-tokyo.ac.jp (L. Stuhl).

https://doi.org/10.1016/j.nimb.2019.05.057
Received 15 January 2019; Received in revised form 1 May 2019; Accepted 21 May 2019
Available online 28 May 2019
0168-583X/

1. Introduction

We started a program [1,2] at the RIKEN Radioactive Isotope Beam Factory (RIBF) aiming to measure the spin-isospin responses of light nuclei along the neutron drip line. The studies of dynamic properties of exotic nuclei, such as giant resonances, which manifest themselves at higher excitation energies (>10–15 MeV) are in the very early stage worldwide. Until recently, only the spin-isospin collectivity in stable isotopes was investigated [3]. There is no available data on spin-isospin collectivity for nuclei with large isospin asymmetry factors, where $(N-Z)/A > 0.25$. We aim to investigate this unexplored region up to $(N-Z)/A = 0.5$.

The charge-exchange (p, n) reactions at intermediate beam energies ($E/A > 100$ MeV) and small scattering angles can excite Gamow-Teller (GT) states up to high excitation energies in the final nucleus, without Q-value limitation [4]. The (p, n) reactions in inverse kinematics are efficient tools to extract the B(GT) strengths of unstable isotopes [5,6]. The combined setup of a low-energy neutron counter and the SAMURAI magnetic spectrometer [7] together with a thick liquid hydrogen target allow us to perform such measurements with high luminosity [8]. In this setup, the neutron detector is used for the detection of the recoil neutrons. The neutron kinetic energies are deduced by the time-of-flight (ToF) technique and SAMURAI is used for tagging the decay channel of the reaction residues. Many relevant decay channels after the charge-exchange reaction can be measured in a single magnetic rigidity setting owing to the large acceptance of the SAMURAI spectrometer. Such a setup, including the WINDS neutron counter [9], was already successfully used in our first (p, n) experiment on ^{132}Sn [10]. It was proven that we can take data on unstable nuclei with quality comparable to those on stable nuclei.

Random gamma background, which mainly arises from the environment, such as beam-line detectors, target and detector frames or room background, cannot be distinguished from the neutrons by ToF information alone. In order to eliminate background events due to gamma rays, we developed the PANDORA (Particle Analyzer Neutron Detector Of Real-time Acquisition) system [11,12], as an upgrade of WINDS. In PANDORA, an additional parameter, the pulse-shape discrimination (PSD) was introduced. PANDORA consists of EJ-276 (former EJ-299-33M and EJ-299-34) plastic scintillator bars [13], which are sensitive to the differences between neutrons and gamma rays [14], and are coupled to a photomultiplier tube (PMTs) [15] at each end. PANDORA has a neutron-gamma discrimination capability comparable to the systems with similar type plastics in the literature [16–18].

At the end of 2017, a ^{6}He(p, n) experiment (H391) with PANDORA was performed in inverse kinematics at the HIMAC facility in Chiba. The performance of our (p, n) setup was evaluated using the good test case of a strong GT transition to ^{6}Li. Recently, our first RIBF experiment (SAMURAI30) with 5 days of beam time at SAMURAI was also performed to study the GT transitions including the GT resonances from the ^{11}Li and ^{14}Be drip line nuclei to the ^{11}Be and ^{14}B nuclei.

The properties of PANDORA and details of the digital readout were reported previously [11,12]. In this work, the status of our project in terms of physics experiments with PANDORA is discussed. After a short introduction, the preliminary result of our pilot measurement on ^{6}He will be presented in Section 2. We report on the setup design, the performance of the digital data-acquisition system and kinematical correlation of detected recoil neutrons. Section 3 is devoted to discuss the experimental setup and preliminary results of SAMURAI30. The summary follows in Section 4.

2. The ^{6}He(p, n) measurement

2.1. Setup

In the ^{6}He$(p, n)^{6}$Li measurement at the SB2 beam course of the HIMAC facility, a secondary beam of ^{6}He at 123 MeV/u was produced through a fragmentation reaction of a 160 MeV/u primary beam of ^{11}B on a 20-mm-thick ^{9}Be production target. The resulting cocktail beam had an average intensity of 2×10^{4} particles/s, containing ^{6}He with 96% purity. Fig. 1 shows the layout of the experimental setup.

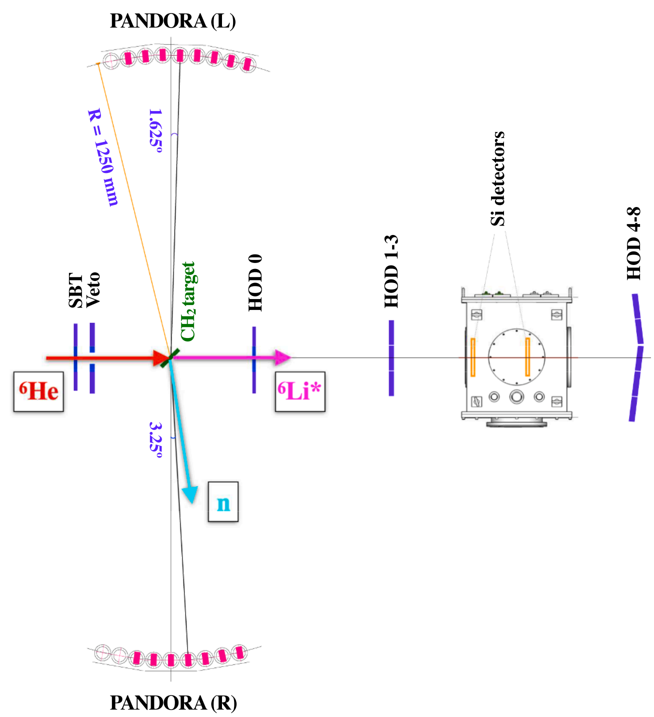

Fig. 1. Experimental setup of the ^{6}He$(p, n)^{6}$Li measurement.

The particle identification (PID) of the beam was performed on an event-by-event basis by using the energy-loss information in the SBT plastic scintillator at the F3 focal point. The secondary beam was impinged on a polyethylene target with 5 mm thickness, rotated by 45°. The recoil neutrons were detected by PANDORA detectors surrounding the target. The left and right walls, with respect to the beam line, covered the angular region of 75°–99° with 3.25° steps.

Hodoscope bars were placed downstream of the target to identify the reaction residues produced by the (p, n) reaction from the incident ^{6}He particles. Depending on the excitation energy, the daughter nucleus, i.e.^{6}Li can decay into multiple reaction residues of light nuclei such as protons, neutrons, tritons, and so on.

With the aim to distinguish such events, the hodoscope setup consisted of three layers; the first layer (HOD 0) was used to identify ^{6}Li only, while the other two layers were segmented along the horizontal axis, HOD 1–3 (3 detector bars in one plane) and HOD 4–8 (5 bars in one plane) so as to facilitate simultaneous detection of light reaction residues and their possible decay products. HOD 0 (HOD 1–8) had a plastic scintillator plate with dimensions of $240^{W} \times 80^{H} \times 2^{D}$ mm^3 ($100^{W} \times 1000^{H} \times 10^{D}$ mm^3). HOD 0 covered the solid angle for ^{6}Li particles emitted with angles up to 7°, which was sufficient to measure the (p, n) reaction at scattering angles up to 15° in the center-of-mass system. Panel (a) of Fig. 2 shows the incoming beam PID on SBT and the gate applied in analysis for ^{6}He particles. Panel (b) of Fig.2 presents the PID of reacted events, generated by the ^{6}He beam, detected in HOD 0. The identified ^{6}Li events are selected with $Z = 3$ gate shown in Fig. 2.

2.2. Data-acquisition system

Data from 15 PANDORA bars (each with a signal from both ends) were read out with a digital data-acquisition system (DDAQ), applying a consumer configured trigger condition. (The trigger will be discussed

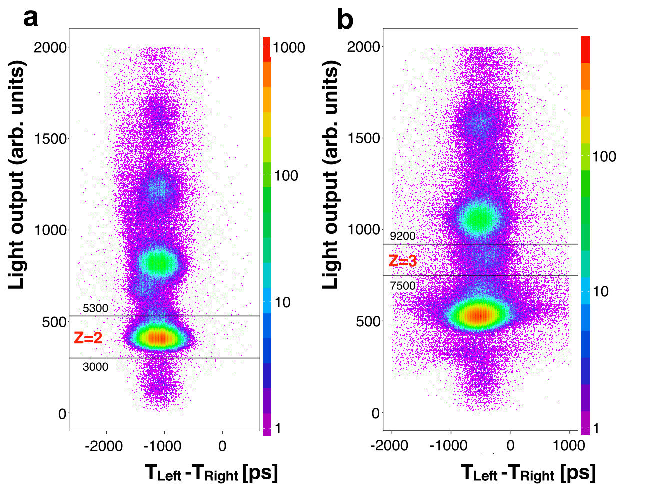

Fig. 2. An incoming (a) and outgoing (b) PID spectrum of the SBT and HOD 0 detectors. The $Z = 2$ and $Z = 3$ gates provided the clear tagging of the ^{6}He(p, n)^{6}Li reaction events.

in more detail in the next paragraph.) The beam line detectors and hodoscopes employed analog readout with analog triggering (DAQ). The read out of the SBT and HOD 0 were duplicated to record their signals in the DDAQ also. For the DDAQ we daisy chained two CAEN V1730B (16-channel modules) and one CAEN V1730D (8-channel module) waveform digitizers using an optical connection. The unpublished software of digiTES, based on Digital Pulse Processing for the Pulse Shape Discrimination (DPP-PSD) firmware [19] was used to manage different modules in the daisy chain condition and control the digitizers. A LUPO (Logic Unit for Programmable Operation) module [20] was used to generate a 62.5 MHz signal to synchronize timestamps of the three modules.

The acquisition in the digitizers was not based on the self-triggering of each channel. The local triggering option of the two-two coupled channels, in V1730 two neighboring channels are paired, was used to ensure the coincidence between the top and bottom PMTs of PANDORA. The digitizers were configured so that the validation of the local triggers came from an external trigger based on the programmed software criteria. In order to manage the coincidence requirements between the SBT start counter, hodoscopes and PANDORA, the first channel (ch 0) of each digitizer was dedicated to a logic signal coming from the coincidence of the start counter and hodoscope detectors (analog DAQ branch). This external trigger was validating the PANDORA self-triggers in a 500-ns wide time window.

2.3. Results

The neutron-gamma discrimination of PANDORA is based on comparison of integrated charges measured over two different time regions of the input signal. The PSD parameter is defined as

$$\mathrm{PSD} = \frac{Q_{Long} - Q_{Short}}{Q_{Long}}, \qquad (1)$$

where Q_{Long} and Q_{Short} are the charges integrated in long (width = 450 ns) and short (width = 42 ns) gates, respectively. The arithmetic mean of PSD values of two single-end readouts of each PANDORA bar (PSD_{bottom} and PSD_{top}) was defined as, PSD_{mean} [11], an additional parameter to the ToF for each event. The combination of the measured neutron ToF with the new PSD parameter improved the discrimination of neutron- and gamma-like events originating from the (p, n) reaction on ^{6}He. Fig. 3 shows the PSD_{mean} plotted against the neutron ToF. The large random gamma background, originating from the environment, in the ToF range of neutrons could not be removed without the PSD information. By using the DDAQ, we were able to detect neutrons having kinetic energies lower than 100 keV.

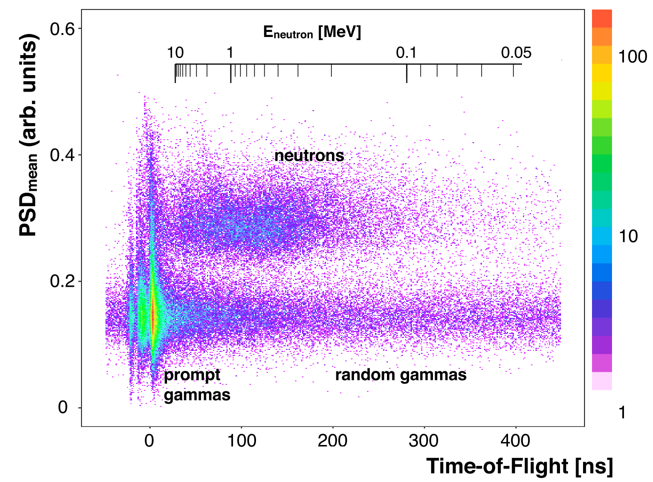

Fig. 3. The PSD_{mean} vs. ToF spectrum of PANDORA shows the importance of separating neutrons and random gamma background. Inset scale corresponds to the kinetic energy of the detected neutrons obtained by the ToF method.

Selecting the incident ^{6}He particles and requiring the identification of ^{6}Li reaction residues produced from the (p, n) reaction and gating on neutron-like events by PSD_{mean}, a clear kinematical correlation can be seen in Fig. 4. This matches with the calculated kinematical correlations for the ^{6}He(p, n) charge-exchange reaction at 123 MeV/u energy and corresponds to transitions to the ground state in ^{6}Li, and demonstrates effectiveness of PANDORA and its PSD capability.

3. The SAMURAI experiment on ^{11}Li and ^{14}Be

3.1. Experimental setup and conditions

The experiment was performed at the RIBF of RIKEN. A secondary cocktail beam of unstable ^{11}Li and ^{14}Be was produced via the fragmentation reaction of a 230 MeV/u ^{18}O primary beam on a 14-mm-thick ^{9}Be target installed at the F0 focal plane of the BigRIPS separator [21]. Two degraders were installed at F1 and F5 with thickness of 5-mm

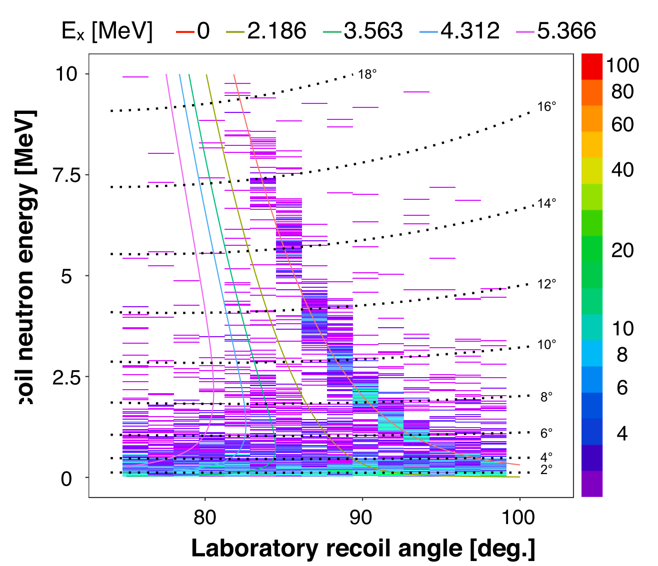

Fig. 4. Correlations between recoil neutron energy and laboratory kinematics for fixed excitation energies. Each vertical bar (a unit in horizontal axis) represents a PANDORA bar.

and 2-mm, respectively. In order to reduce the beam contamination by tritons (as their production rate is much higher than that of nuclei of interest), a special collimator was installed in the beam line.

Fig. 5 shows a schematic view of the experimental setup around the SAMURAI spectrometer. Downstream of STQ25, two 1-mm-thick plastic scintillators (SBT1,2) were installed for the detection of beam particles. The SBTs were used to produce the beam trigger (threshold was set to $Z > 2$). The beam PID was performed on an event-by-event basis by measuring the energy loss in SBTs and the ToF of the beam particles in BigRIPS between F7 and F13.

Downstream from the SBTs, two multi-wire drift chambers were installed (BDC1,2) for measuring the trajectories of the beam particles.

The secondary cocktail beam consisted of ^{11}Li at 182 MeV/u with intensity of 2.5×10^5 particle/s and ^{14}Be at 198 MeV/u with intensity of 1×10^5 particle/s with purity of 48% and 19%, respectively. The triton contamination was below 30%. The secondary beam was transported onto a 10-mm-thick, 60-mm diameter liquid hydrogen (LH) target (rotated by 45°) at the secondary target position of SAMURAI (F13).

The neutron detector setup on the left and right sides of the LH target consisted of 27 PANDORA plastic scintillators and 13 additional scintillator bars of WINDS. The distance between the LH target and PANDORA or WINDS was around 125 cm. Each detector was placed such that the 25-mm-wide (PANDORA) or 30-mm-wide (WINDS) plane faced the target. The left and right wings with respect to the beam line covered the laboratory recoil angular region of 47°–113° and 62°–134°, respectively, with 3.25° steps. PANDORA was optimized to detect neutrons with a kinetic energy of 0.1–5 MeV. The time reference for the ToF was taken from SBT1,2. The threshold for the light output in the scintillator was set to be 60 keV$_{ee}$, corresponding to 200 keV proton energy. All bars had duplicated readout; CAEN V1730 modules were used for charge and PSD information while an analog circuit was used for timing and triggering.

The reaction residues entered into SAMURAI after passing through the forward drift chamber, FDC0. The magnetic field of the spectrometer was set to 2.75 T. At the focal plane of SAMURAI, a wall (HODF24 detector) of 24 plastic scintillator bars with dimensions of $1200^W \times 100^H \times 10^D$ mm^3 was installed, to measure the trajectories, energy loss, and ToF (from SBTs) of the reaction residues. Further downstream, an additional wall (HODP device) with 16 plastic bars (same as HODF24 bars) was installed. Those bars (the 3rd and 4th) of HODF24 which were hit by the unreacted beam were excluded from trigger. Fig. 6 shows a typical PID spectrum detected in HODF24 for events generated by the ^{11}Li or ^{14}Be beams. The reaction products and decay particles can be clearly identified. NEBULA was used to detect the fast decay neutrons of the reaction products (decays by 1n and 2n emissions).

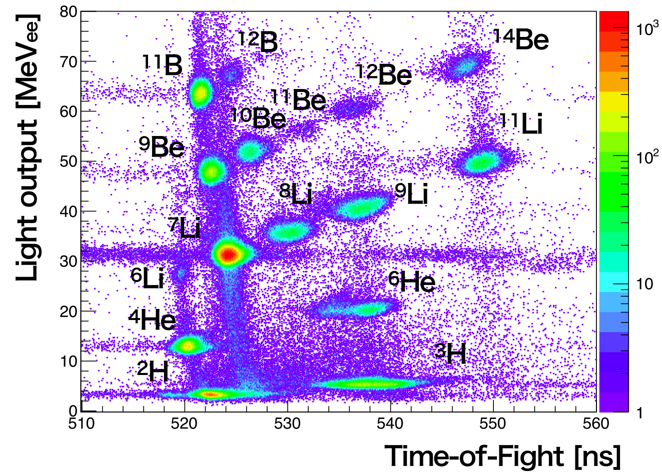

Fig. 6. A PID spectrum in the focal plane of SAMURAI spectrometer, measured by one bar (bar ID = 7) of HODF24.

In this experiment, the DDAQ of PANDORA was configured in a similar way as described in Section 2.2., except for the trigger validation signal on the first channels (ch 0) of CAEN V1730B and V1730D digitizers. The validation signal originated from the triple coincidence of "BEAM" (from SBT detectors) and analog "PANDORA" (recoil neutron) and "HODOSCOPE" (reaction residues at hodoscopes). The typical trigger rate was 1.3×10^3 Hz.

3.2. Neutron-gamma separation and preliminary results

Fig. 7 shows the two-dimensional plot of PSD$_{mean}$ vs. total light output of a PANDORA bar for events associated with ^{11}Li beam. Clear separation of neutron-like events even at the low-light output region is observed. To evaluate the PSD performance of PANDORA, the Figure-of-Merit (FoM) based on the projections of the PSD$_{mean}$ spectra was used:

$$\mathrm{FoM} = \frac{\Delta_{\gamma-n}}{L_{\gamma-FWHM} + L_{n-FWHM}}, \tag{2}$$

where ($\Delta_{\gamma-n}$) is the PSD difference between the neutron and gamma component peaks, and $L_{\gamma-FWHM}$ and L_{n-FWHM} are the full widths at half maxima of the gamma and neutron distributions, respectively. In this work, the window method [11] was used to calculate the FoM. Panels

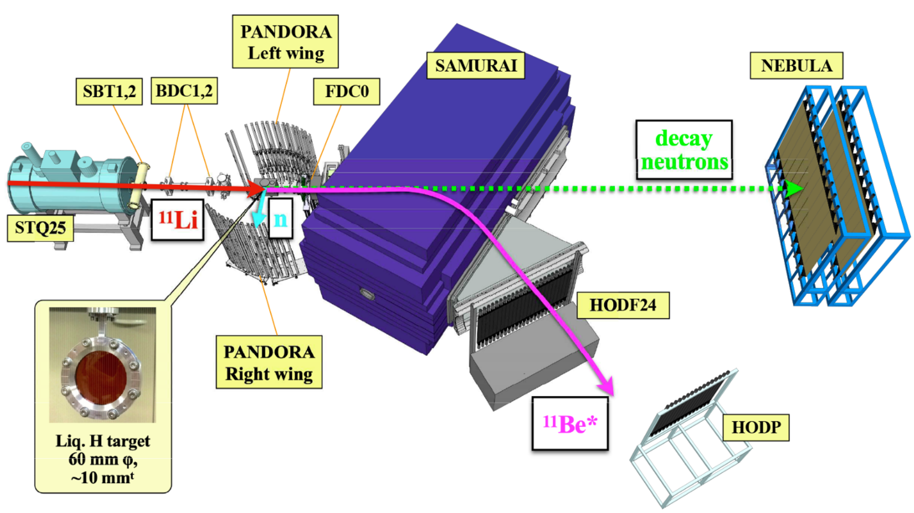

Fig. 5. The schematic view of the experimental setup around the SAMURAI spectrometer.

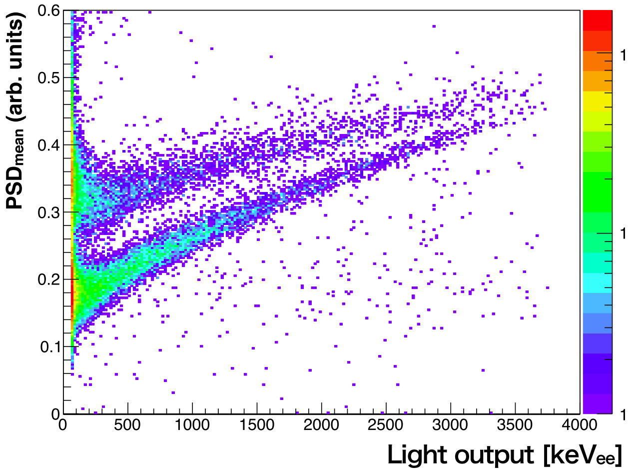

Fig. 7. PSD_{mean} as a function of total light output (bar ID = 7). Signals from neutrons are located in the upper distribution of the graph, whereas signals from gamma rays are in the lower band.

(a), (b), (c), and (d) of Fig. 8. present the projected PSD_{mean} distributions of neutron- and gamma-like events, with 200-keV_{ee} wide window centered at light outputs of 300 keV_{ee}, 500 keV_{ee}, 900 keV_{ee}, and 1500 keV_{ee}, respectively. The FoM values are 1.17 ± 0.02 (a), 1.22 ± 0.01 (b), 1.28 ± 0.01 (c), and 0.98 ± 0.02 (d). We obtained higher FoM values than those reported in the literature for similar materials [16–18].

Fig. 9 shows the plot of kinetic energy as a function of laboratory scattering angle for recoil neutrons associated with the ^{11}Li beam. We required the simultaneous detection of ^{9}Li and d in HODF24 and neutron detection in PANDORA (offline PSD cut was applied). A clear kinematical correlation between the measured kinetic energy and the laboratory scattering angle, above 18 MeV excitation energy, was obtained. This forward scattering peak (2°-7° in the center-of-mass system) suggests a GT transition. The $^{9}Li + d$ decay channel of ^{11}Be is observed for the first time. Reconstruction of the excitation-energy spectrum up to about 30 MeV, including the GT giant resonance region, is ongoing.

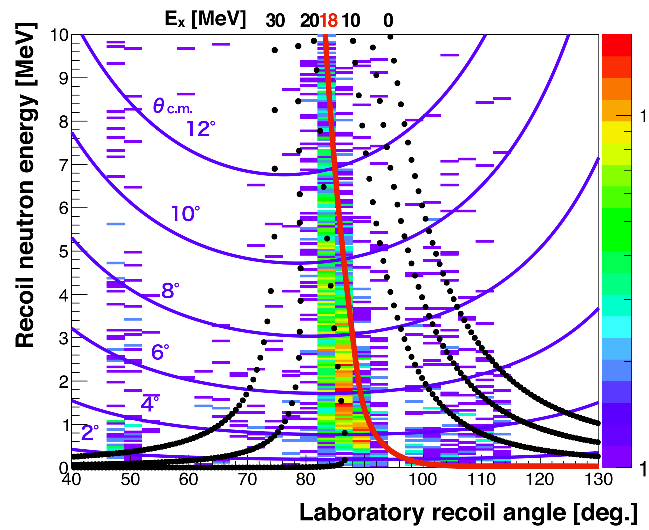

Fig. 9. Neutron spectra as a function of recoil neutron energy and scattering angle in the laboratory frame, using the right wing of PANDORA setup.

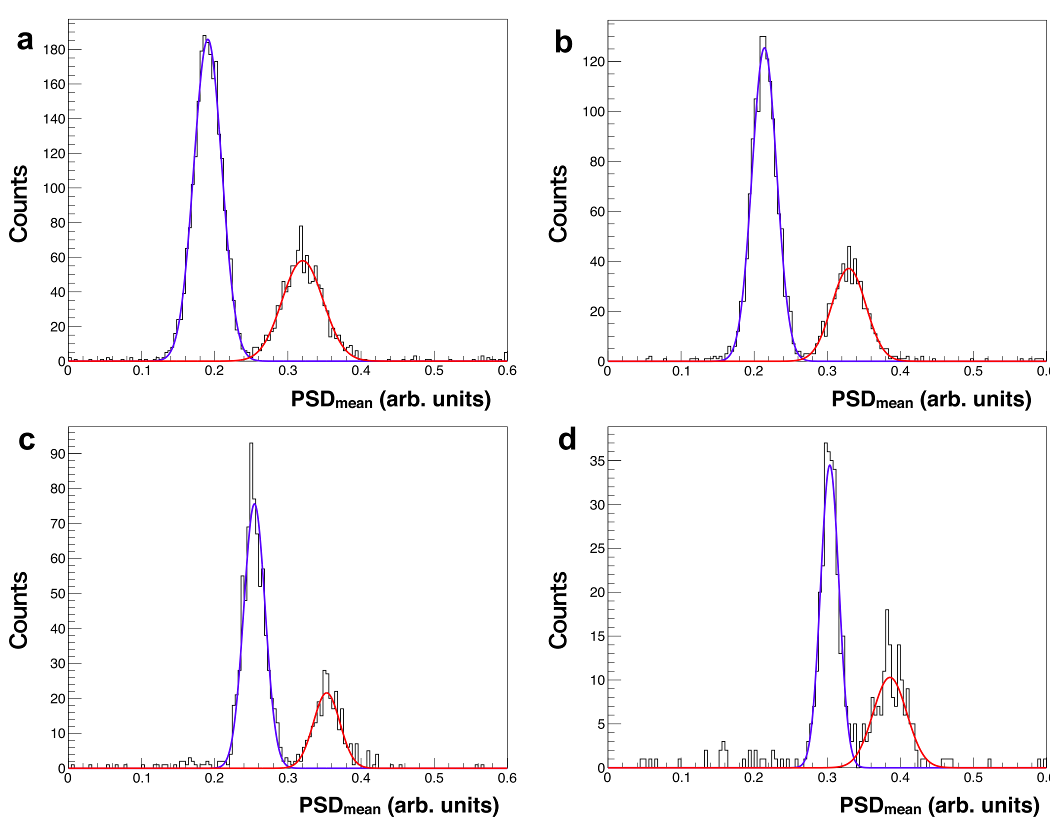

Fig. 8. Panels (a), (b), (c), and (d) present the projected PSD_{mean} distributions of neutron- and gamma-like events, with 200-keV_{ee} wide window centered at light outputs of 300 keV_{ee}, 500 keV_{ee}, 900 keV_{ee}, and 1500 keV_{ee}, respectively. The FoM values are 1.17 ± 0.02 (a), 1.22 ± 0.01 (b), 1.28 ± 0.01 (c), and 0.98 ± 0.02 (d).

4. Summary

The neutron-gamma discrimination capability of our new low-energy neutron detector, PANDORA, was demonstrated with the ^{6}He(p, n)^{6}Li reaction in inverse kinematics at the HIMAC facility. The transition to the ground state in ^{6}Li daughter nucleus was observed. PANDORA and its digital data-acquisition system were combined with the standard analog data acquisition of SAMURAI in order to perform (p, n) reactions in inverse kinematics for light, neutron drip line nuclei for the first time. In the ^{11}Li(p, n)^{11}Be and ^{14}Be(p, n)^{14}B reactions, PANDORA was used for detecting recoil neutrons and SAMURAI was used for tagging the decay channel of reaction residues. The neutron-gamma discrimination performance was evaluated by the experimental data using FoM. We obtained higher FoM values than those reported in the literature. Preliminary results were reported. From the ^{11}Be generated by ^{11}Li(p, n) reaction, the exotic decay channel of $^{9}Li + d$ was observed, using PANDORA.

Acknowledgments

We express our gratitude to the RIKEN and CNS staff for the stable operation of the accelerators during the measurement. The authors are thankful to HIMAC accelerator crew for their efforts and support. This work was supported by the Japan Society for the Promotion of Science, the KAKENHI project 16H06716 and the China scholarship Council. It was also partially supported by a Kurata Grant from the Kurata Memorial Hitachi Science and Technology Foundation, NKFIH (Gr. No. NN128072) and ÚNKP-18-4-DE-449 New National Excellence Program of the Human Capacities of Hungary. G. G. Kiss acknowledges support form the János Bolyai research fellowship of the Hungarian Academy of Sciences. Z. H. gratefully acknowledges the support provided by the Hungarian Academy of Sciences under Grant No. NN114454-NKFIH. This work was supported by the Rare Isotope Science Project of Institute for Basic Science funded by Ministry of Science and ICT and NRF of Korea (2013M7A1A1075764).

References

[1] K. Yako, et al., RIKEN Accel. Prog. Rep. 45 (2012) V.
[2] L. Stuhl, et al., RIKEN Accel. Prog. Rep. 48 (2015) 54.
[3] K. Nakayama, et al., Phys. Lett. B 114 (1982) 217.
[4] T.N. Taddeucci, et al., Nucl. Phys. A 469 (1987) 125.
[5] M. Sasano, et al., Phys. Rev. Lett. 107 (2011) 202501.
[6] M. Sasano, et al., Phys. Rev. C 86 (2012) 034324.
[7] T. Kobayashi, et al., Nucl. Instrum. Methods Phys. Res. B 317 (2013) 294.
[8] J. Yasuda, et al., Nucl. Instrum. Methods Phys. Res. B 376 (2016) 393.
[9] K. Yako, et al., RIKEN Accel. Prog. Rep. 45 (2012) 137.
[10] J. Yasuda, et al., Phys. Rev. Lett. 121 (2018) 132501.
[11] L. Stuhl, et al., Nucl. Instrum. Methods Phys. Res. A 866 (2017) 164.
[12] L. Stuhl, et al., Proceedings of Science (INPC2016) 085.
[13] EJ-276 Plastics Datasheet:https://eljentechnology.com/products/plastic-scintillators/ej-276.
[14] N. Zaitseva, et al., Nucl. Instrum. Methods Phys. Res. A 668 (2012) 88.
[15] Hamamatsu H7195 Datasheet:https://www.hamamatsu.com/eu/en/product/alpha/P/3002/H7195/index.html.
[16] S.A. Pozzi, et al., Nucl. Instrum. Methods Phys. Res. A 723 (2013) 19.
[17] D. Cester, et al., Nucl. Instrum. Methods Phys. Res. A 735 (2014) 202.
[18] P. Blanc, et al., Nucl. Instrum. Methods Phys. Res. A 750 (2014) 1.
[19] Digital Pulse Processing for the Pulse Shape Discrimination (DPP-PSD):http://www.caen.it/csite/CaenProd.jsp?parent=39&idmod=770.
[20] LUPO Datasheet:https://ribf.riken.jp/RIBFDAQ/index.php?DAQ/Information/Module/LUPO.
[21] N. Fukuda, et al., Nucl. Instrum. Methods Phys. Res. B 317 (2013) 323.